

# Viscoelasticity of a protein monolayer from anisotropic surface pressure measurements

P. Cicuta<sup>1,a</sup> and E.M. Terentjev<sup>2</sup>

<sup>1</sup> Nanoscience Center, University of Cambridge, J.J. Thomson Avenue, Cambridge CB3 0FF, UK

<sup>2</sup> Cavendish Laboratory, University of Cambridge, Madingley Road, Cambridge CB3 0HE, UK

Received 16 August 2004 / Received in final form 28 October 2004

Published online 22 February 2005 – © EDP Sciences, Società Italiana di Fisica, Springer-Verlag 2005

**Abstract.** We present a method to completely characterize the viscoelasticity of Langmuir monolayers. In contrast to existing techniques, both the compression and shear moduli are determined at the same time, in a single experiment and with a standard apparatus. This approach relies on the measurement of anisotropy in the surface pressure: the tension is measured in orientations perpendicular and parallel to the compression direction. We apply this technique to the study of  $\beta$ -lactoglobulin spread monolayers, a system that has been shown to develop a shear modulus at high concentration.  $\beta$ -lactoglobulin monolayers are interesting both because of their importance in food science and because they exhibit universally slow dynamical behavior that is not fully understood. Our results confirm that the compressional modulus dominates the total viscoelastic response and also provide a complex shear modulus, emerging above a critical concentration. We are able to describe how each of the dynamical response moduli is related to the surface concentration and to the equilibrium osmotic pressure.

**PACS.** 83.60.Bc Linear viscoelasticity – 68.18.-g Langmuir-Blodgett films on liquids – 64.70.Pf Glass transitions

## 1 Introduction

Experimental probes for the study of monolayer rheology have not yet been developed as fully as rheometers to characterize complex fluids in the bulk. This has caused a lag in the study of these systems, and in particular of polymer dynamics in two dimensions (2d) as compared to bulk polymer solutions. The restricted dimensionality of the interface strongly reduces the available configurations for these systems. This can be expected to affect the mechanical and viscoelastic properties in a dramatic way. For this reason we are interested in the dynamics of insoluble macromolecules confined to two dimensions.

In this paper we present a new method for probing the linear viscoelastic response of a monolayer. Our approach has the main advantage of being very simple and relying only on a standard apparatus available in any surface science laboratory: the Langmuir trough and Wilhelmy plate tensiometer, however used in a non-standard way. We apply this method to study of  $\beta$ -lactoglobulin monolayers, finding surprising results for the elastic response moduli as a function of the surface concentration: we interpret these effects as a liquid to solid transition that occurs through steric jamming.

There are excellent reviews on the mechanical behavior of proteins at interfaces [1–3] and also specifically on spread protein films [4]. The protein we study here is the archetypical  $\beta$ -lactoglobulin. It contains 162 amino acids and has a molecular weight of about 18 kDa. The molecule contains 2 disulfide and 1 free sulfhydryl groups, and in the bulk it is globular with a well-defined secondary structure. In solution at room temperature  $\beta$ -lactoglobulin can be found in diversely aggregated forms depending on the pH. A reason that motivates extensive interest in  $\beta$ -lactoglobulin is its relevance in food science: it accounts for 58% of the whey proteins in milk. It is strongly amphiphilic, therefore, its presence plays an important part in determining the interfacial properties in milk-based systems. An example of practical importance is the control of droplet coalescence in oil/water emulsions. This is a process that reduces the interfacial area, so coalescence can occur only if the film is compressed or the molecules are forced out of the interface. Since both these effects require energy, protein films provide a very efficient, cheap and bio-compatible emulsion stabilizing mechanism. Their surface properties also play a role in other physical processes like foaming, thickening and gelling.

In recent work we have studied a number of aspects of equilibrium and dynamical behavior in the two main proteins present in milk:  $\beta$ -casein [5] and  $\beta$ -lactoglobulin [6].

<sup>a</sup> e-mail: pc245@cam.ac.uk

These proteins generally unfold to a considerable degree when they adsorb at the air/water or oil/water interfaces [1]. In monolayers of these proteins, at low concentration, we found a polymer-like 2d semidilute regime, and verified that the mechanical properties of these systems are in many ways analogous to the behavior of monolayers made of neutral synthetic homopolymers [6]. In the present work we focus on high concentrations of protein adsorbed on the interface, near close packing. The central result is the emergence of complex shear modulus above a certain critical concentration, prompting questions about the mechanisms of aggregation in 2d. We discuss our findings in context of the existing knowledge on polymer monolayers. In particular very slow stress relaxation is seen in many polymer monolayers and the reasons for it are not fully understood. This has been motivating a lot of recent work addressing polymer dynamics on slow timescales (frequencies  $\omega \lesssim 1$  Hz) [7, 8].

This paper is organized as follows. Section 2 contains a brief recap of principles of 2d rheology and its particular application for our method of measurement of anisotropic surface pressure, the analysis of which allows us extraction of new information about the system. Specific descriptions of the materials, the experimental techniques and analysis are the subject of Section 3. The results, presented in Section 4, are divided into groups for compressional and shear response, at low and high concentrations of surface protein. Here some discussion accompanies the results, however it is in Section 5 (Discussion) that we attempt to bring all the results and our understanding together, as well as to make contact with other studies and results in the literature. Finally, in Conclusions we summarize the work and outline the questions for future work.

## 2 Viscoelasticity in monolayers

In a classical Langmuir trough experiment, the surface tension  $\gamma$  is measured as a function of concentration  $\Gamma_{\text{surf}}$  of the polymer adsorbed on the interface. As the concentration increases the tension falls, and this change can be seen as a lateral osmotic pressure  $\Pi_{\text{eq}} = \gamma_0 - \gamma$ , where  $\gamma_0$  is the tension of the free interface [9].

The response to a deformation in an isotropic 2d material is characterized in general by two elastic moduli: changes in area are controlled by the compression modulus  $\varepsilon$  (often referred to as dilation modulus in the trade) and changes in shape by the shear modulus  $G$  [10]. In order to introduce our particular measurement technique, we now very briefly review the notation and experimental methods used in surface rheology, pointing to the reviews by Miller et al. [10] and Joly [11] for further detail.

The mechanical response to compressions is proportional to the compression elastic modulus  $\varepsilon$ . If the compression is very slow (quasi-static) then an equilibrium modulus is probed, which can be measured from the slope of a pressure-area isotherm

$$\varepsilon_{\text{eq}} = -A \frac{\partial \Pi_{\text{eq}}}{\partial A}, \quad (1)$$

where  $A$  is the surface area and  $\varepsilon_{\text{eq}}$  is the inverse of a compressibility. If the compression speed is finite, then there might be friction resisting the compression flow, and the resistance is characterized by the compression (dilational) viscosity  $\eta_d$ , defined as:

$$\eta_d = A \frac{\Pi - \Pi_{\text{eq}}}{\frac{d}{dt}A}. \quad (2)$$

In effect, equations (1-2) define the real and imaginary parts of the complex dynamic compression modulus.

In practice, and traditionally in the field of study of adsorbed monolayers, one is more interested in looking at concentration dependence. The surface concentration on the interface is simply related to the area, through  $\Gamma_{\text{surf}} = M/A$ , with  $M$  the total mass of the material deposited on the interface (assumed constant for “insoluble” monolayers). Obviously decreasing the area increases the surface concentration, and the measurement of  $\varepsilon = -A(\partial \Pi / \partial A)$ , equation (1), directly translates into

$$\varepsilon = \Gamma_{\text{surf}}(\partial \Pi / \partial \Gamma_{\text{surf}}).$$

### 2.1 Linear viscoelasticity

When a monolayer is both elastic and viscous, a common measurement consists in oscillating the surface area (this being the strain variable in the problem) sinusoidally around  $A_0$ , so

$$A(t)/A_0 = 1 + \delta A(t)/A_0 = 1 + \Delta A/A_0 \cos \omega t, \quad (3)$$

where  $\Delta A$  is the amplitude and  $\omega$  the frequency of imposed area oscillation. The pressure  $\Pi$  is measured as function of time. If the response is linear, then  $\Pi$  will be found to oscillate with a certain phase shift compared to the area oscillation:

$$\Pi(t)/\Pi_0 = 1 + \Delta \Pi / \Pi_0 \cos(\omega t + \varphi). \quad (4)$$

If the layer is purely elastic, then area and pressure are in phase; if it is purely viscous, then they are 90 degrees out of phase. It is a common notation to define the frequency dependent complex modulus  $\varepsilon^*(\omega)$ :

$$\varepsilon^*(\omega) = \varepsilon'(\omega) + i\varepsilon''(\omega) = \varepsilon'(\omega) + i\omega \eta_d(\omega). \quad (5)$$

Here the real part is the elastic storage component of the modulus:  $\varepsilon' = |\varepsilon^*| \cos \varphi$ ; the imaginary part is the dissipative component:  $\varepsilon'' = |\varepsilon^*| \sin \varphi$ .

As in bulk rheology, the shear elastic modulus  $G$  is defined as the ratio between the increment of shear stress in response to the shear strain increment; the shear elastic viscosity  $\eta_s$  is the ratio between the shear stress and the rate of shear. In the same way, in an oscillatory measurement one can measure the complex shear modulus:

$$G^*(\omega) = G'(\omega) + iG''(\omega) = G'(\omega) + i\omega \eta_s(\omega). \quad (6)$$

In principle, measuring the stress relaxation  $\Pi(t)$  following an instantaneous step of strain also provides a complete characterization of the rheology of a material, equivalent to a set of measurements of the complex modulus in oscillatory strain as a function of frequency.

## 2.2 Measuring the compressional modulus

In important processes like emulsification and foaming, the main deformations are compression and expansion of the interface [12]. For this reason a lot of effort has gone into developing experimental geometries to probe this elastic modulus specifically. One approach is the design of Langmuir troughs with custom-made compression barriers to achieve isotropic compressions [13]. Another method has become popular and relies on assembling the layer on a pendant drop and on varying the volume of liquid in the drop. This is assumed to achieve the isotropic expansion and compression of the surface, and by imaging the gravity-distorted profile of the pendant drop, the surface tension can be recovered as a function of area.

The simplest, and also the most common method of studying the complex dilational (compression) modulus is to perform oscillatory compressions of the film with the Langmuir trough barriers, measuring the surface pressure and the phase shift between the tension signal and the surface area. It is well known that by performing such uniaxial compressions the film is actually subject to both compression and shear. Indeed it can be shown that the response is nominally determined by the sum of the compression and shear moduli. The contribution from the shear modulus is usually overlooked, under the (often well-justified) assumption that it will be negligible compared to the compression modulus. For example in polymer monolayers in the semidilute regime, both the real and imaginary components of the dynamic shear modulus are indeed negligible, at least at low frequencies [14, 15].

Techniques exist that rely on studying the dynamics of surface waves. These waves may be either externally generated, like Excited Capillary Waves (ECW), or thermal, like in Surface Quasi-Elastic Light Scattering (SQELS). Both these techniques are probing the response to uniaxial compressions and thus measure the combined compression and shear modulus.

## 2.3 Measuring the shear modulus

The shear modulus describes the response of the system to changes in shape that occur at constant area. A common geometry relies on detecting the angular displacement and torque on a rotating disk sitting in the plane of the surface. There are commercially available instruments to measure surface shear with this method. One important limitation is that it is very difficult to accommodate this geometry into a Langmuir trough, making concentration dependent studies difficult in practice. Adsorbed protein films, very similar to the ones investigated in the present work, have been recently studied in [16] with a device of this type. There are also numerous other custom built designs. A particularly successful surface shear rheometer images the linear displacement of a thin needle in a linear open-channel geometry [17]. This device can be integrated into a Langmuir trough, and also has the advantage of minimizing the contribution of the sub-phase on the motion of the moving elements, making the

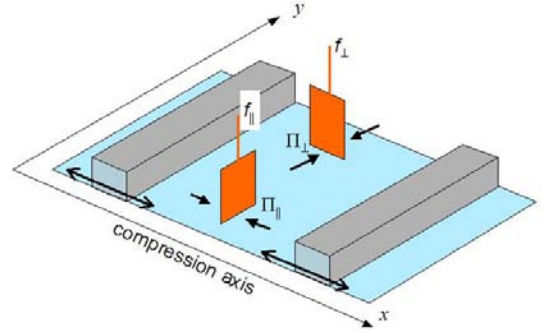


**Fig. 1.** Geometry of the compression in the Langmuir trough. The two barriers compress the monolayer symmetrically with small oscillatory movements in the  $x$ -direction. The distance between the barriers and the Wilhelmy plates is typically around 8 cm. A microbalance measures the force  $f$  that the monolayer exerts on the Wilhelmy plates, corresponding to the surface pressure parallel ( $\Pi_{\parallel}$ ) and perpendicular ( $\Pi_{\perp}$ ) to the compression direction.

apparatus particularly sensitive. Another instrument was described recently, in which the motion of a rigid disk dragged through a monolayer is interpreted through the solution of this corresponding hydrodynamic problem [18].

We have developed a method that does not require two different experimental geometries for the separate measurement of the compression and shear modulus. On the contrary, we choose a uniaxial compression geometry, Figure 1, where the response is a combination of these moduli, and then show how each component can be recovered. It was recently demonstrated by Petkov et al. [19] that in dense monolayers an anisotropy in surface pressure can be detected through surface tension measurements performed with different plate orientations. It is this effect that can be used to measure the shear modulus of monolayers.

Starting from the general expressions for a homogeneous viscoelastic medium, and within the limits of a linear viscoelastic response, Petkov et al. showed explicitly how to obtain the principal components of the stress tensor  $\tau_{xx}$  and  $\tau_{yy}$ , as a function of the uniaxial strain applied in the  $x$ -direction:

$$\begin{aligned}\tau_{xx} &= \Pi_{\parallel} - \Pi_0 = (\varepsilon' + G')\alpha + (\eta_d + \eta_s)\dot{\alpha} \\ \tau_{yy} &= \Pi_{\perp} - \Pi_0 = (\varepsilon' - G')\alpha + (\eta_d - \eta_s)\dot{\alpha},\end{aligned}\quad (7)$$

where  $\alpha$  is the relative dilation:

$$\alpha = \ln \frac{A(t)}{A_0} \simeq \frac{\delta A(t)}{A_0} \quad \text{and} \quad \dot{\alpha} = \frac{\partial \alpha}{\partial t}.\quad (8)$$

For the oscillatory deformation  $\delta A(t)/A_0 = \Delta A/A_0 \cos \omega t$  considered above, equation (7) becomes:

$$\begin{aligned}\delta \Pi_{\parallel}(t) &= \frac{\Delta A}{A_0} \left[ (\varepsilon' + G') \cos \omega t + \omega(\eta_d + \eta_s) \sin \omega t \right] \\ \delta \Pi_{\perp}(t) &= \frac{\Delta A}{A_0} \left[ (\varepsilon' - G') \cos \omega t + \omega(\eta_d - \eta_s) \sin \omega t \right].\end{aligned}\quad (9)$$

In [19] this theoretical description was used to show that adsorbed protein films develop a finite shear modulus. The experiments were performed at a single frequency, and were aimed at studying the fluidizing effect of added surfactant. Neither the frequency dependence or the dissipative components of the elastic moduli were investigated. We apply the framework of equation (9) to study both the real and dissipative components of the compressional and shear moduli, within the range of frequencies allowed by our experimental setup. By choosing to study a spread monolayer system we can vary the area per monomer, thus identifying several critical concentrations at which the system undergoes major dynamic transformations.

### 3 Experimental methods

#### 3.1 Materials

$\beta$ -lactoglobulin (Sigma, L-0130, bovine milk, mixture A and B types, min.90% pure, lot. 91H7005) is used as supplied. 1 mg/ml solutions in deionized water are prepared from the dried, powdered protein, stored in a refrigerator and used within 4 days. Buffer solutions are made up using deionized (Elgastat UHQ, Elga, U.K.) water. Phosphate buffer 0.02M is used to control the  $pH$  at 7.1, and NaCl 0.02M is added to control ionic strength. Monolayer material is spread on the liquid/air interface by careful dropwise addition ( $\simeq 0.5\mu l$ ) of the spreading solution with a Hamilton syringe.  $\beta$ -lactoglobulin is spread in dilute conditions, and left to equilibrate for 10–15 minutes.

#### 3.2 Langmuir trough

We control the monolayers within a Langmuir trough (mod. 610, Nima Technology, U.K.) and measure the surface pressure using a microbalance sensor (type PS4, Nima Technology, U.K.). We have measured the response time of these sensors by instantaneously loading them with 10 mg and 2 mg weights. This response time is between 0.1 s and 0.2 s, which is negligible compared to the timescales of the slow dynamics that will be discussed in the remainder of the paper. We use a Wilhelmy plate of 1 cm width, made of filter paper. Once the filter paper is pre-soaked in the subphase liquid, a very reproducible contact angle ( $\simeq 0^\circ$ ) is established and confirmed visually. The whole apparatus is enclosed in a draught proof enclosure. Before spreading, the surface is compressed and the top layer of the subphase is aspirated with a pipette. We verify that the surface is clean by checking that the pressure rise between fully expanded and fully compressed is  $\lesssim 0.1$  mN/m.

In all of the experiments discussed in this paper, proteins are spread in dilute conditions or at very low pressures ( $\leq 2$  mN/m). This is to ensure that the initial amount of overlap between different chains, which might become permanent and could act as cross-links, is negligible. The concentration is then increased by using the Langmuir trough barriers to reduce the available surface area [20]. In this way, given that the chains are effectively

irreversibly adsorbed to the interface, proteins remain segregated from each other. Figure 1 shows the geometry of our setup. Notice in particular that the compression is achieved with two symmetrical barriers, and that the pressure sensors are positioned at the mid-distance. To minimize dynamical effects and get the closest possible to an equilibrium measurement, we compress the monolayer at the slowest continuous speed enabled by our hardware: the area change is  $\sim 5$  cm<sup>2</sup> per minute, corresponding to a strain rate of between 2 and  $8 \times 10^{-4}$  s<sup>-1</sup>.

A special rigid hook holding the Wilhelmy plates ensures that their orientation does not change in time. An effect of the orientation of the plate with respect to the barrier motion is sometimes reported in the literature, usually for very concentrated films. This may be purely an artifact, indicating a wrongly conducted measurement. For example, in reference [21] it is noted that for concentrated  $\beta$ -casein films the surface pressure measured with the parallel plate was smaller than with a perpendicular plate ( $\Pi_{\parallel} < \Pi_{\perp}$ ). This was done with a one-barrier trough, and this geometry cannot prevent that for a sufficiently rigid film the concentration around the Wilhelmy plates may become inhomogeneous. The film has stopped flowing “behind” the plate, and the pressure reading loses significance. In our own laboratory, we clearly saw this effect in preliminary experiments on  $\beta$ -lactoglobulin conducted with a one-barrier trough (“asymmetric” compression). We even observed that at high concentration ( $\Pi \geq 8$  mN/m) the film became sufficiently rigid to drag the plate along. It is clear that as soon as the monolayer compression modulus becomes high, or a shear modulus develops, it becomes necessary to perform symmetric compressions, with two-barrier troughs.

#### 3.3 Oscillatory measurements

As described in Section 2.3, by performing dynamical experiments we can probe both the storage and dissipative components of the compression and shear moduli. A typical measurement is illustrated in Figure 2. Here the surface pressure is recorded as function of time, as the area is changed by imposed oscillatory barrier movements. The surface pressure is measured with two Wilhelmy plates at orthogonal orientations, giving the values in directions parallel ( $\Pi_{\parallel}$ ) and perpendicular ( $\Pi_{\perp}$ ) to the compression axis. It can be clearly seen from the plot that  $|\Pi_{\parallel} - \Pi_0| > |\Pi_{\perp} - \Pi_0|$ . This is the signature of a finite shear modulus, cf. equations (9). It can also be seen that the surface pressure precedes the strain, as expected for a material with a finite dynamic viscosity (loss modulus). In this example the oscillation frequency is 0.016 Hz, the average pressure  $\Pi_0 = 15.6$  mN/m,  $\Delta\Pi_{\parallel} \simeq 0.5$  mN/m,  $\Delta\Pi_{\perp} \simeq 0.4$  mN/m,  $\Delta A/A_0 = 0.6\%$  and the phase lag is  $\delta t = 2.9$  s.

In a typical experiment, data points are recorded every 0.5 s. Traces comprising around 20 oscillation cycles are saved for each frequency. This data is then analyzed by finding the set of times  $\{t_{A,i}\}$  at which the area value is  $A_0$  and the set of times  $\{t_{\Pi,i}\}$  at which the pressures

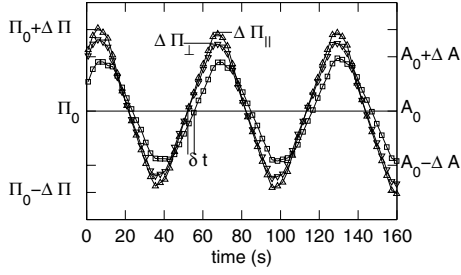


**Fig. 2.** The surface pressure recorded as function of time, as the area ( $\square$ ) is changed by oscillatory barrier measurements. The surface pressure is given in two orthogonal orientations,  $(\Pi_{\parallel}, \Delta)$  and  $(\Pi_{\perp}, \nabla)$  with respect to the compression direction. Note that  $|\Pi_{\parallel} - \Pi_0| > |\Pi_{\perp} - \Pi_0|$ , indicating a finite shear modulus, as discussed in the text.

are  $\Pi_0$ . Then the value of  $\delta t$  is calculated as the average of the difference between each of the time-set values:  $\delta t = \langle t_{A,i} - t_{\Pi,i} \rangle_i$ . A set of  $\{t_{\Pi,i}\}$  is acquired for orthogonal and parallel orientations of the barriers, from which two values  $\delta t_{\perp}$  and  $\delta t_{\parallel}$  are obtained. These are so close that their difference cannot be detected by eye in the raw signals of Figure 2. The value of the frequency is calculated as  $\omega = 0.5 / \langle t_{A,i+1} - t_{A,i} \rangle_i$ . This approach is better suited to our data as compared to a Fourier-analysis of the traces, because it does not require a long term stability (coherence) of the oscillations.

Given that each value of time will have an error of  $\pm 0.25$  s and that the set of times contains around 40 values, we estimate that the resolution in  $\delta t$  is around  $\pm 0.05$  s. We hold the amplitude of oscillation at a constant value, with  $\Delta A/A_0$  between 0.6 and 1.5%. Martin et al. [16] have shown that the response is linear up to 4% in adsorbed  $\beta$ -lactoglobulin films. The range of barrier velocities in our present experimental setup is limited: at a fixed oscillation amplitude of around 2%, a frequency range between 0.01 and 0.25 Hz is possible. This corresponds to oscillation periods  $T$  between 4 s and 100 s. Given the experimental conditions discussed above, the theoretical resolution in determining  $\delta t/T$  is then 1%, in the worst case. This can be improved by averaging over more oscillation periods.

The values of  $\Delta A$  and  $\Delta \Pi$  are then extracted from the data traces by calculating the average of the difference between the maximum and minimum values. We define the maxima and minima as the mid-points between passing through the average value. The uncertainty in our analysis is calculated from the standard deviations in each of the averaging procedures described above.

From these values we calculate:

$$\begin{aligned} |\varepsilon^* + G^*| &= A_0 \frac{\Delta \Pi_{\parallel}}{\Delta A} \\ |\varepsilon^* - G^*| &= A_0 \frac{\Delta \Pi_{\perp}}{\Delta A}. \end{aligned} \quad (10)$$

The phase angle  $\vartheta$  is equal to  $2\pi\omega\delta t$  and the elastic and dissipative components of the response are obtained

from:

$$\begin{aligned} \varepsilon' + G' &= |\varepsilon^* + G^*| \cos \vartheta \\ \varepsilon' - G' &= |\varepsilon^* - G^*| \cos \vartheta \\ \varepsilon'' + G'' &= |\varepsilon^* + G^*| \sin \vartheta \\ \varepsilon'' - G'' &= |\varepsilon^* - G^*| \sin \vartheta. \end{aligned} \quad (11)$$

We have first performed the experiments with two pressure sensors measuring at the same time, as shown in Figure 1. This is how our experience could be described. We have repeated every experiment after having rotated both the Wilhelmy plates by  $90^\circ$ , taking care to match all other experimental parameters (spreading amount, age of layer, frequency values, etc.). To our surprise it was found that one of our two sensors had a slower response time and thus the comparison of the dynamical data between two sensors was impossible. In this paper we report results obtained with the single sensor, from repeated experiments in two different geometries. It is clear that with two identical sensors, the simultaneous measurement of pressures would result in a technique that is both more practical and precise.

### 3.4 Analysis of time scales

While of course a driving system could be constructed to extend the frequency range towards higher frequencies, it is worth pointing out that there are fundamental problems that would then complicate the experiments considerably. Indeed the simple treatment of the monolayer, as summarized in Section 2.3, treats the film like a homogeneous material, implicitly assuming that propagation of strain occurs on much faster timescales than the dynamical processes described above. To consider the validity of this approximation, an estimate of the time necessary to propagate the strain over the entire monolayer is required. The speed of the compression wave is surprisingly low in monolayers, and we shall see that the higher frequencies of our experiments are already at the limit where the propagation time has to be taken into account. This is illustrated in Figure 3, where the “raw data” time intervals  $\delta t$  (defined as explained in Fig. 2) are plotted as a function of the barrier oscillation period. It can be seen that as the period becomes shorter, the values of  $\delta t$  fall and would eventually reach zero. A part of this trend is due to the finite time that the compression wave takes to travel from the barriers to the pressure sensors. This gives rise to a delay that erodes the phase difference between pressure and area oscillations. This delay becomes more important the higher the frequency.

Quantifying this effect is not trivial. Lucassen and van den Tempel [22] have studied the propagation of compression waves in monolayers. This requires a complex experiment in which the surface pressure oscillations are monitored as a function of the separation from the barriers. They have shown that in the case of a purely elastic surface the wave velocity is

$$v \simeq \varepsilon' \sqrt{\frac{\omega}{\eta\rho}}. \quad (12)$$

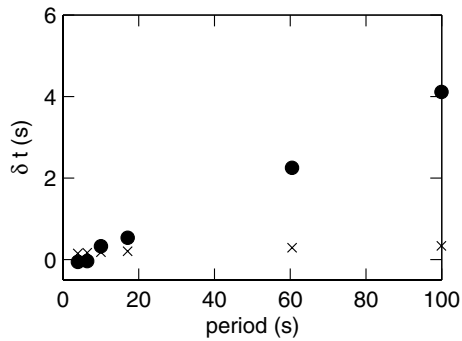


**Fig. 3.** The “raw” values (●) of the time-shift between the pressure and area curves, for a set of experiments at the same monolayer conditions but different oscillation frequencies. Also shown (×) are the compression wave propagation times  $\tau_{\text{prop}}$ , obtained from equation (12). The comparison shows that for long oscillation periods it may not be necessary to consider  $\tau_{\text{prop}}$ , but it does become important at higher frequency. The data shown here correspond to the conditions indicated in Figure 2.

This formula is the dispersion relation that describes a wave of frequency  $\omega$ , driven by the surface elasticity (compression modulus  $\varepsilon'$ ) and damped by a subphase of viscosity  $\eta$  and density  $\rho$ . It applies to waves propagating away from an oscillating barrier in an infinite half-plane. Typical velocities  $v$  are between 5 cm/s and 30 cm/s for the conditions used in this work. The approximation of a purely elastic layer is closely satisfied by most monolayers, because the elastic components of the elastic modulus are usually much larger than the dissipative ones. Knowing the distance between the barriers and the pressure sensors, we can use equation (12) to calculate the propagation time  $\tau_{\text{prop}}$ . Unfortunately equation (12) cannot be directly applied to our experiments because in our geometry the compression is symmetric, hence the monolayer velocity relative to the subphase is zero in the middle of the trough. For this reason the dissipation due to the subphase is overestimated by equation (12), so  $\tau_{\text{prop}}$  is also overestimated. We can consider the propagation time predicted by equation (12) as an upper bound, knowing that in our geometry the propagation time will be smaller. In Figure 3  $\tau_{\text{prop}}$  is plotted together with the experimental “raw” values of  $\delta t$ . It can be seen that the correction due to the wave propagation speed is almost negligible at low frequency and becomes important only at the higher frequencies. However, because of the linear dependence on the elastic modulus in equation (12), any phase difference between the signals will eventually be dominated by the propagation time for a low enough modulus. For the lowest frequency of our experiments, we find that the two timescales become similar around  $\Pi_0 \simeq 4.5$  mN/m. Below this pressure, we cannot use the simple treatment described here. From calibrations with other samples (DMPC phospholipid monolayers) that exhibit little dissipation at low frequencies [10], we estimate that in our geometry the propagation time is between a third and a half of the value given by equation (12). We apply  $\tau_{\text{prop}}/3$  as correction to the values

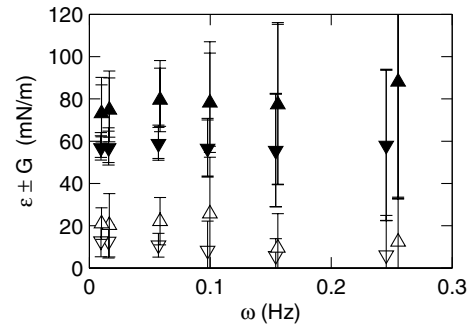


**Fig. 4.** Typical values of the total elastic response of the monolayer:  $\varepsilon' + G'$  (▲);  $\varepsilon' - G'$  (▼);  $\varepsilon'' + G''$  (Δ);  $\varepsilon'' - G''$  (▽). The monolayer conditions are the same as in Figures 2 and 3. As described in the text, the mean of the filled symbols is the compression modulus elasticity, and the mean of the open symbols is the compression modulus dissipation. The semi-difference of the symbols are respectively the shear elasticity and dissipation.

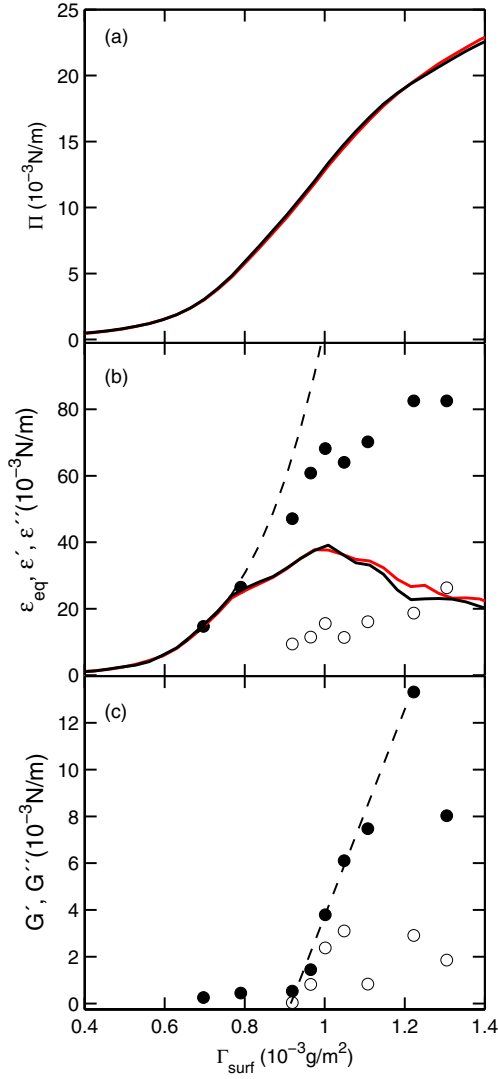
of  $\delta t$  before calculating the phase angles  $\vartheta$  as described above.

Figure 4 shows the frequency dependence of the four components of the response, obtained by using equations (11) and having included the correction for propagation time. To summarize, it should be noted that the phase differences found in this study are always very small angles. Their precise determination and the issue of the consideration of propagation time do not affect (to first order) the values of the real components of the elastic response (both compression and shear). This correction also plays no role in establishing a difference between orthogonal plate orientations. However it does become essential if the frequency dependence of the dissipative components is to be studied in detail, and we shall address this topic in future work.

## 4 Results

Figure 5a presents the equilibrium surface pressure isotherms, obtained by very slow continuous compression of the surface monolayer. The pressure isotherms measured with continuous symmetric compression are independent of the Wilhelmy plate orientation, within the experimental error, and the two separate curves for  $\Pi_{\parallel}$  and  $\Pi_{\perp}$  in Figure 5a are indistinguishable. This equilibrium pressure isotherm is taken as a reference curve, so that we can use the value of pressure  $\Pi(A)$ , or equivalently  $\Pi(\Gamma_{\text{surf}})$ , to recover the value of concentration in different experiments.

The set of results shown in Figure 4 is representative of the frequency dependence seen at all the pressures and concentrations explored in this work. The surface moduli are nearly independent of frequency, at least within our experimental error which can be seen to be quite large. We have interpolated the frequency dependent results to obtain uniform data at 0.1 Hz at each concentration. These results are shown in Figures 5b and c, as a function of surface concentration  $\Gamma_{\text{surf}}$ . The interpolated values shown in



**Fig. 5.** (a) Surface pressure as a function of the surface concentration,  $\Pi_{\parallel}(\Gamma_{\text{surf}})$  and  $\Pi_{\perp}(\Gamma_{\text{surf}})$ . Two lines overlap to a very good approximation, showing that this equilibrium modulus is isotropic. (b) Solid lines are the equilibrium compression modulus  $\varepsilon_{\text{eq}}$ , obtained from the isotherms shown in panel (a) using equation (1); (●) and (○) are respectively the elastic  $\varepsilon'$  and viscous  $\varepsilon''$  components of the dynamic compressional response. The dashed line is the power-law  $\varepsilon \sim \Gamma_{\text{surf}}^{5.5}$ . (c) Dynamic shear moduli as function of  $\Gamma_{\text{surf}}$ , (●):  $G'$  and (○):  $G''$ . The dashed line shows that the shear elastic modulus grows approximately linearly with the concentration, above  $0.91 \text{ mg/m}^2$ .

Figure 5 are essentially an average over about 6 frequency-dependent values, so the error (not shown) is roughly half the error in the single measurements of Figure 4.

## 4.1 Compression modulus

### 4.1.1 Low concentrations and semidilute regime

Monolayers of  $\beta$ -lactoglobulin have a range of concentrations, corresponding to pressures of a few mN/m, where

the surface pressure and the compression modulus  $\varepsilon_{\text{eq}}$  both show a very clear scaling behavior as a function of concentration. This behavior is typical of flexible polymers in 2d, and is the evidence that the protein chains are unfolded at the interface. In this approximation, the chain conformation can be statistically described by the Flory exponent  $\nu$ : if the monomer size is  $a$  and the number of monomers per chain is  $N$  then the radius of gyration of the polymer is [23]:

$$R_g \simeq aN^{\nu}. \quad (13)$$

Note that a random polymer coil strictly confined in 2d has a very different topology from the usual 3-dimensional chains, in that chain interpenetration is nearly impossible and they generally do not share the same physical volume, as in 3d.

At very low surface concentration the monolayer is in a dilute regime: a gas of polymer chains confined to the surface. The surface pressure and elasticity in this regime are too low to be studied with our apparatus. A “semidilute” regime begins above the concentration  $\Gamma_{\text{surf}}^*$  where individual chains would be forced to overlap. The corresponding non-dimensional fraction of monomers on the surface is  $\Phi^* = \Gamma_{\text{surf}}^* a^2 / [\text{monomer mass}]$ . From the simple argument, that at this point all of the available area  $A$  is occupied by chains of surface area  $R_g^2$ , it follows that the overlap concentration scales as

$$\Phi^* \simeq N^{1-2\nu}. \quad (14)$$

The equilibrium properties of polymers in the semidilute regime are given by scaling laws, with exponents related to  $\nu$ . In particular both the osmotic pressure and the equilibrium compression modulus scale like:

$$\Pi_{\text{eq}} \simeq \frac{k_B T}{R_g^2} \left( \frac{\Gamma_{\text{surf}}}{\Gamma_{\text{surf}}^*} \right)^{y_{\text{eq}}} \quad \text{and} \quad \varepsilon_{\text{eq}} \sim \Gamma_{\text{surf}}^{y_{\text{eq}}}, \quad \text{where } y_{\text{eq}} = 2\nu/(2\nu - 1). \quad (15)$$

This was first demonstrated experimentally in reference [24]. Many protein systems follow the relation of equation (15), up to a limiting pressure that lies typically between 2 and 7 mN/m [1]. This scaling behavior of the compression modulus is shown by the dashed line in Figure 5b, and a value of exponent  $y_{\text{eq}} = 5.5$  is found for our system. This corresponds to Flory exponent  $\nu = 0.61$ , which is intermediate between an ideal ( $\theta$ -condition) chain and a chain in good solvent ( $\nu = 0.75$  in 2d).

The range of concentration where the monolayer is in the semidilute regime and equation (15) holds is found between  $0.37 < \Gamma_{\text{surf}} (\text{mg/m}^2) < 0.75$ . From the lower value for the overlap concentration  $\Gamma_{\text{surf}}^*$ , and using equation (13) assuming that the proteins are chains with  $N = 162$  (the number of residues in a  $\beta$ -lactoglobulin molecule), we can extract an area per monomer of  $a^2 \simeq 18 \text{ \AA}^2$ . This is in good agreement with the expected monomer size, considering that  $3.5 \text{ \AA}$  is the known repeat distance in a  $\beta$ -sheet motif. This confirms the picture of the monolayer as a semidilute solution of flexible polymers with excluded

volume constraint. We can therefore use equation (14) to estimate that area fraction covered by monomers at the onset of the semidilute regime is  $\Phi^* \approx 0.32$ . Note that while relative changes in concentration obtained by compressing the layer are very precise, the absolute value of the concentration is only known to within  $\pm 15\%$ .

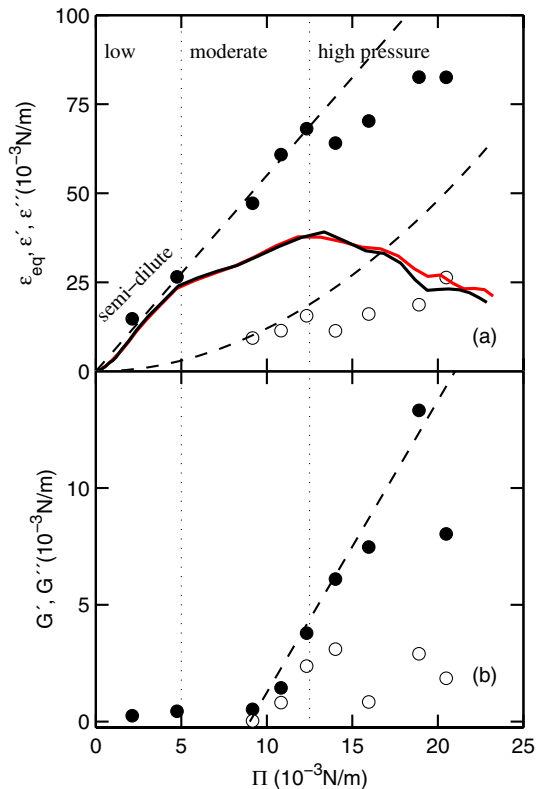
Within the semidilute regime, the experimental values of  $\varepsilon'$  and  $\varepsilon_{\text{eq}}$  are indistinguishable. This can be seen in Figure 5b for  $\Gamma_{\text{surf}}$  up to  $0.75 \text{ mg/m}^2$ . In Figure 5 we only show data from experiments reproduced by re-orienting the surface sensors and matching conditions. We have much more additional data from either of the two orientations, that can be used to measure the compression modulus while the shear modulus is negligible. This extensive data (not shown) confirms the full agreement between  $\varepsilon'$  and  $\varepsilon_{\text{eq}}$ .

Figure 6a shows the compression moduli plotted as function of the surface pressure. This representation is particularly useful to identify any regions where the elastic moduli and the pressure have the same dependence on the concentration, because in these regions there will be a linear relation between the variables, see equation (15). In Figure 6a, below the pressure of  $5 \text{ mN/m}$  (that corresponds to  $\Gamma_{\text{surf}} = 0.75 - 0.8 \text{ mg/m}^2$ ), both  $\varepsilon'$  and  $\varepsilon_{\text{eq}}$  depend linearly on the pressure. A line of slope 5.5 is seen to interpolate this data very well, indicated by the dashed line. It directly follows from the equation (15) and the definition of  $\Pi$ , that the slope of the linear relationship is given by the power-law exponent  $y_{\text{eq}}$ ,  $\varepsilon = y_{\text{eq}}\Pi$ . This exponent is also independently obtained from the  $\Pi(\Gamma_{\text{surf}})$  curve fitting. Note that, although the equilibrium modulus  $\varepsilon_{\text{eq}}$  is only linear within the boundaries of semidilute regime, the dynamic storage modulus  $\varepsilon'$  ( $\bullet$  symbols) remains so significantly into the region of solid packing.

The compression viscosity, represented by the loss modulus  $\varepsilon''$  at constant frequency ( $\circ$  symbols), does not follow a linear function of pressure. Such a linear relationship would imply viscosity values significantly larger than zero at low pressures. This does not follow from our data, although, as discussed above, our measurement of viscosity at low pressures is affected by the compression wave propagation time. We suggest that the data is interpolated very well by a parabola, indicated by the second dashed line in Figure 6a. The choice of this scaling may appear arbitrary, however, it is motivated by the recent discovery that for a wide range of polymer monolayers the compression viscosity scales with a power of the concentration that is twice the exponent found for the pressure and the elasticity,  $\eta_{\text{d}} \sim \Gamma_{\text{surf}}^{2y_{\text{eq}}}$  [6]. This would indeed imply that the dynamic viscosity would be a quadratic function of the pressure,  $\eta_{\text{d}} \sim \Pi^2$ , at least in the semidilute regime.

#### 4.1.2 Moderate and high concentrations

At concentrations above  $\Gamma_{\text{surf}} = 0.8 \text{ mg/m}^2$ , that is pressures  $\Pi > 5 \text{ mN/m}$ , the equilibrium and dynamical moduli have significantly different values, with  $\varepsilon' > \varepsilon_{\text{eq}}$ . The continuing linear dependence  $\varepsilon'(\Pi)$ , at least until  $\Pi = 12.5 \text{ mN/m}$ , is extremely surprising, because in this



**Fig. 6.** (a) Solid lines are the equilibrium compression modulus  $\varepsilon_{\text{eq}}$ , obtained from continuous slow compression of the monolayer, as a function of the surface pressure  $\Pi$  (the two lines correspond to  $\Pi_{\parallel}$  and  $\Pi_{\perp}$  orientations). Data symbols ( $\bullet$ ) and ( $\circ$ ) are respectively the elastic  $\varepsilon'$  and viscous  $\varepsilon''$  components of the dynamic compressional response. Dotted lines identify the regimes of low, moderate and high pressures, as described in the text. (b) Dynamic shear modulus response as a function of  $\Pi$ , ( $\bullet$ ):  $G'$  and ( $\circ$ ):  $G''$ .  $G'$  grows linearly with pressure from  $\Pi = 9 \text{ mN/m}$ .

same region ( $0.75 < \Gamma_{\text{surf}}(\text{mg/m}^2) < 1$ ) neither the pressure and  $\varepsilon_{\text{eq}}$ , nor  $\varepsilon'$ , lie on the same power laws of the concentration that held at lower concentrations, as can be seen by the deviations from the low concentration fit shown in Figure 5b by the dashed line. We return to this delicate point in the discussion section.

At even higher concentrations the apparent  $\varepsilon_{\text{eq}}$  begins to decrease with concentration. Here the dynamic modulus  $\varepsilon'$  also drops slightly, before resuming an approximately linear dependence on the surface pressure. The last data point at the highest pressure  $\Pi \simeq 20 \text{ mN/m}$  is probably anomalous, very likely due to collapse of the monolayer into the subphase.

#### 4.2 Shear modulus

A shear viscoelastic response develops in the compressed protein monolayer at a concentration  $\Gamma_{\text{surf}} \simeq 0.9 \text{ mg/m}^2$ , just above the value where the equilibrium and dynamical compression moduli begin to differ from each other. We would like to emphasize that the difference of this value

and the upper boundary of semidilute regime, albeit small, is significant and unambiguous. We do not attribute it to the low detection threshold, because after its emergence the shear elastic modulus is approximately linear both in concentration, see Figure 5c and in pressure, Figure 6b. A linearity as a function of concentration has also been observed in other soft 3D systems, like emulsions compressed above the random close packing concentration [25].

These results on the shear modulus are in excellent quantitative agreement with measurements on spread monolayers of  $\beta$ -lactoglobulin conducted very recently [14] with a customized interfacial rheometer, under very similar conditions to this study. This is a very significant confirmation that the method presented here for measuring the shear modulus is as effective as a dedicated instrument.

The shear modulus results presented here can also be compared to measurements on adsorbed protein layers. Adsorbed layers are reported to have shear moduli  $10 < G'(\text{mN/m}) < 21$  for  $54 < \varepsilon'(\text{mN/m}) < 98$  [19]. Another very recent study shows that the  $\varepsilon'$  vs.  $\Pi$  curves for adsorbed  $\beta$ -lactoglobulin layers [26] are practically indistinguishable from the ones obtained here in spread layers. Also the values of the shear modulus obtained in that study are in agreement with our work:  $G' \simeq 10$  mN/m at  $\varepsilon' \simeq 100$  mN/m. The conformation of adsorbed and spread monolayers is not necessarily the same, but their viscoelastic response appears to be very similar.

The dissipative shear component  $G''$  also develops at the same pressure as the storage modulus  $G'$ . After the initial onset, in the regime of high compression we find that the shear response is predominantly elastic  $G'' \ll G'$ . At present it is premature to speculate on the detailed dependence of  $G''$  on concentration given the quality of this early data.

### 4.3 Aging behavior

In many adsorbed protein layers, viscoelasticity strongly depends on the monolayer age. We have carried out a preliminary investigation of aging in the system studied here. After spreading in dilute conditions, as described above, the monolayer was compressed to achieve the target pressure. We have chosen three points:  $\Pi = 12$ ,  $\Pi = 14$  and  $\Pi = 19$  mN/m (cf. Fig. 6). The linear viscoelastic response of these monolayers was measured at different times after reaching the target pressure: 10 min, 1, 3, 5 and 22 h. The compression and shear moduli were extracted from each data set as described in the previous sections. We found no definite trends in these moduli as a function of age, and in particular – no dramatic growth in the shear moduli, as has been reported by various groups for adsorbed layers of  $\beta$ -lactoglobulin [16] and other globular proteins [27].

## 5 Discussion

The behavior of dynamic compression modulus at low pressures (in the semidilute regime of the monolayer) confirms the results on concentration dependence that have

been obtained recently with a completely different technique (SQELS) [6]. Firstly, the elastic (storage) modulus  $\varepsilon'$  scales with the same power law of concentration as the osmotic pressure, and we can thus conclude that the effect is due to the entropic cost of confining the random polymer chains in 2d. Secondly, the compression viscosity (loss modulus  $\varepsilon''$ ) scales with twice this power-law exponent, a result that is not fully understood but nevertheless is likely determined by the statistical properties of the semi-dilute regime. SQELS probes thermal fluctuations of very small amplitude and high frequency, and could only be used at low values of the elastic moduli, essentially restricting the investigated range to the semidilute regime [28]. The agreement at low pressures between these two techniques is very satisfactory, as it confirms that both are probing equilibrium properties in the regime of linear response. The anisotropic Langmuir trough technique presented here is more robust than SQELS, and the results extend far beyond the semidilute regime, up to very high concentrations.

A protein monolayer develops a shear modulus, that is, becomes a nominal solid, as a result of developing a contact network. This can equivalently be thought of as the appearance of energy barriers preventing either the whole proteins or parts of the polymeric chain from flowing under thermal excitations. In a colloidal model system, a shear modulus can develop from one of two processes: either the formation of links (bonds) between different particles, driven by attractive interactions and leading to a branched percolating structure, or the dynamical arrest due to crowding, where each particle is effectively caged by the neighboring hard-core repulsive interactions [29].

It is known both from simulations of hard-disk objects in 2d [30] and from experiments on confined colloidal particles [14] that at area fractions around  $\Phi \simeq 0.8$  these systems undergo a full kinetic arrest driven by the hard-core repulsion. In the  $\beta$ -lactoglobulin layers presented here, the equilibrium and dynamical response to compression differ above the surface density  $\Gamma_{\text{surf}} \simeq 0.8$  mg/m<sup>2</sup>. Assuming the simple approximation that the area of surface covered by each polymer is  $a^2N$  (simply meaning  $N$  objects of the area  $a^2$  each), this concentration corresponds to an area fraction  $\Phi \simeq 0.53$ . This estimate is certainly crude, and also we do not have a physical probe to determine the detailed molecular conformation, so it would be misleading to compare this number with the results for ideal hard-disks. We should however note that this indicates a relatively high coverage. This means that it is quite possible that the system is undergoing a kinetic arrest because of steric jamming; the development of a shear modulus and the very slow relaxation dynamics may all be consequences of this dynamical transition.

It should be noted that in the existing literature on protein monolayers, and on  $\beta$ -lactoglobulin layers in particular, this scenario is not proposed. Slow dynamics and relaxations are often attributed to conformation changes or very slow desorption [31,32]. The growth of a shear modulus, and more generally the solid-like behavior has been previously linked to the development of a network

of bonds, that is the formation of a gel through local attractive interactions [33]. In the case of adsorbed proteins, the surface film is often multi-layer and intermolecular bonds are observed with various spectroscopic techniques [34]. In a complex system like a protein monolayer various processes will take place, and it is difficult to find direct evidence for or against each hypothesis. In the case of a spread layer, we would however find it difficult to understand why a cross-linked gel should only begin to form at  $\Gamma_{\text{surf}} \gtrsim 0.9 \text{ mg/m}^2$ , when the proteins already had a significant window of concentrations where they were held in close contact under compression (staring at  $\Gamma_{\text{surf}}^* \approx 0.37 \text{ mg/m}^2$  in our system). Our results suggest that no significant effect of bonds established between segments of protein molecules takes place in a compressed monolayer. Simulations of 2d networks of spherical particles have shown that the presence of irreversible flexible bonds can lead to the emergence of anisotropy in the pressure when the system is uniaxially compressed [35]. This pressure anisotropy is qualitatively similar to the results of our experiments. The simulations show that it can happen even for very low values of the concentration, provided that the bonds form a percolating structure. As already mentioned above, our experiments only show anisotropy above a high threshold concentration. The simulation result itself does not prove the necessity of inter-molecular bonds, on the contrary the same simulations also show that, at very high density of spheres, even a system of non-bonded particles will exhibit an anisotropic stress response. This is closer to what we believe is happening in the protein monolayer. The simulations therefore validate the idea that the development of a shear modulus could be determined by the close-packing of hard-cores leading to jamming. It would be naïve to compare quantitatively these simulations with the experiments reported here, because within the simulation each protein is approximated as a smooth sphere, whereas a compressed 2D polymer is a rough object whose movements are subject to more constraints.

We now put forwards an argument to estimate the concentration at which we expect the emergence of a shear modulus, above the onset of the semidilute region of compressed chains. Classically, the scaling description of semidilute concentrations requires that chains are no longer regarded individually. The whole system is treated as a collection of monomers, whose connectivity only matters at increasingly small length scales: the total length of polymer chains does not have any effect [23]. To understand shear response in a monolayer we need once again to consider individual chains. In the 2d compressed state it is known that chain interpenetration is low for topological reasons. Therefore we can approximate each chain as a (deformable) disk, that has been compressed to a radius  $R < R_g$ . Shear is by definition an area-conserving deformation. However microscopically it has to be achieved by deformations of individual chains, that will carry a free energy cost. Let us assume for simplicity that a shear strain  $\sigma$  induces a deformation that is equivalent to a local additional compression. Then each chain reduces its area from

$\pi R^2$  to  $(1 - \sigma)\pi R^2$ . From equation (15) we can write the free energy per chain:

$$F \simeq \left(\frac{R}{R_g}\right)^2 k_B T \left(\frac{\Gamma_{\text{surf}}}{\Gamma_{\text{surf}}^*}\right)^{y_{\text{eq}}} \equiv k_B T \left(\frac{\Gamma_{\text{surf}}}{\Gamma_{\text{surf}}^*}\right)^{y_{\text{eq}}-1}. \quad (16)$$

We can now estimate the free energy cost per chain due to a strain  $\sigma$ :

$$\Delta F = k_B T \left[ \left(\frac{1}{1 - \sigma}\right)^{y_{\text{eq}}-1} - 1 \right] \left(\frac{\Gamma_{\text{surf}}}{\Gamma_{\text{surf}}^*}\right)^{y_{\text{eq}}-1}. \quad (17)$$

This expression of the free energy penalty per chain explicitly depends on the applied strain, on the concentration (relative to the overlap concentration  $\Gamma_{\text{surf}}^*$ ) and on the Flory exponent  $\nu$  (through  $y_{\text{eq}}$ ). When the chains are compressed to the point that  $\Delta F \geq k_B T$ , they can be regarded as hard disks, no longer able to deform and therefore jammed – hence the emergence of the shear elastic modulus. Taking the measured values  $y_{\text{eq}} = 5.5$ ,  $\Phi^* = 0.32$ ,  $\Gamma_{\text{surf}}^* = 0.37 \text{ mg/m}^2$ , together with the typical strain of  $\sigma = 1\%$ , we find from equation (17) that the onset of shear should occur at  $\Gamma_{\text{surf}} = 0.73 \text{ mg/m}^2$ . This is reasonably close to the measured value ( $\sim 0.9 \text{ mg/m}^2$ ), considering the crude level of this estimate. Let us point out that equation (17) predicts a non-trivial emergence of the shear modulus above a critical strain. It also follows that for a fixed strain of 1% the shear modulus will be negligible while  $\Gamma_{\text{surf}}/\Gamma_{\text{surf}}^* \leq 7$  in good solvent conditions ( $y_{\text{eq}} = 3$ ), and in a more restricted region  $\Gamma_{\text{surf}}/\Gamma_{\text{surf}}^* \leq 1.45$  for  $\theta$ -solvent conditions ( $y_{\text{eq}} \simeq 8$ ). These predictions, as well as the dependence of critical concentration on strain, could be tested in future on other polymer monolayers.

The difference between the equilibrium compression modulus  $\varepsilon_{\text{eq}}$  and the dynamical elastic modulus  $\varepsilon'$  above  $\Gamma_{\text{surf}} = 0.75 \text{ mg/m}^2$  is striking and significant. It almost certainly is the result of emerging long-time relaxation dynamics in the system, giving rise to an additional elastic component at frequencies higher than the inverse relaxation time. However we want to point out a subtle aspect of the observed behavior: the dynamic modulus  $\varepsilon'$  maintains the linear dependence on  $\Pi_{\text{eq}}$  that was characteristic of the equilibrium semidilute regime, in a region where  $\Pi_{\text{eq}}$  itself has long lost the power-law functional dependence on the concentration. The only picture we can suggest to make these two facts consistent is that in equilibrium (given only thermal excitations) the protein chains become progressively trapped above  $\Pi = 5 \text{ mN/m}$  (the end of semidilute regime), and the system loses its ergodicity. Then the entropic cost of further confinement does not grow with concentration as fast as in the semidilute fluid. The equilibrium modulus loses the classical power-law dependence on concentration because of freezing-out of some conformations. On the other hand, under the small dynamical strain excitations imposed by the oscillating barriers, the proteins (or any 2d polymer chains) are now forced to explore all chain configurations, even their thermally-frozen fraction. In other words the suggestion is that under induced oscillating deformations the free energy landscape

still has the same concentration-determined features as in the fluid regime.

This scenario suggests a number of connections with other model systems where dynamical transitions are well known, and also calls for specific experiments to look for characteristic dependencies on perturbation length scale and frequency that are expected for the response functions.

Lastly we would like to point out that very recent work on polymer monolayers by various authors shows similar effects to the  $\beta$ -lactoglobulin monolayers studied here. In particular in poly(vinylacetate) monolayers, for which the air/water interface is a good solvent (in terms of the Flory exponent for the radius of gyration), Monroy et al. reported the development of a shear modulus at low temperature, above a critical pressure [36]. The pressure dependence of the complex compressional modulus was also explored. On a different system (poly(4-hydroxystyrene)), for which the air/water interface is a poor solvent, the development of complex relaxation dynamics was observed by either compressing the layer above a threshold pressure or upon lowering the temperature. These results are discussed as evidence of a glass transition [8]. These experiments suggest to us that there is very likely a shared underlying physics describing the onset of a shear modulus and the appearance of complex relaxation dynamics in protein and polymer monolayers. Conversely, the establishing of a percolating network of chemical bonds (as the main mechanism of shear response) must be very system-specific and not universal as the proposed connections.

## 6 Conclusions

We have presented a method for fully characterizing the mechanical properties of a Langmuir monolayer, by measuring both the compression and shear modulus in a single experiment. Our approach is based on standard apparatus and therefore we expect that it may find widespread use. The frequency range that is accessible is relatively narrow ( $0.01 < \omega < 0.1$  Hz), but this is comparable to other surface rheometers.

We have used this technique to study the compression and shear elastic response in spread layers of  $\beta$ -lactoglobulin. We find quantitative agreement with existing data on similar systems, and in addition we have found and discussed the functional dependence of each dynamic modulus on the concentration. Throughout the concentration range, the response is dominated by the storage component of the compressional modulus, and also for shear elasticity the storage component is dominant:  $\epsilon' > \epsilon'' > G' > G''$ . At relatively low concentrations we find a classical 2d semidilute regime, where the shear modulus is zero and both the storage and dissipative components of the compressional modulus follow characteristic power laws of the concentration. This behavior breaks down above a threshold pressure, a behavior that we have argued is consistent with a dynamical arrest transition whereby the system becomes progressively non-ergodic. At a next threshold pressure, a finite shear modulus begins

to evolve, this being a further evidence that the concentration is high enough for the direct interaction between the hard core elements of the protein chains to come into play forming a network structure. We have argued that there is no evidence here for attractive bond-like interactions.

We have discussed our results in the wider context of polymer monolayers, showing that there are a number of common universal features. The fact that simpler and more controlled synthetic homopolymer systems may exhibit (some of) the same behavior should be of interest for the food science community. On the other hand a more detailed study of some of the effects described in this work poses a renewed challenge for novel experimental investigations.

We thank the IRC for Nanotechnology and EPSRC for funding of this project.

## References

1. D. Möbius, R. Miller, *Proteins at liquid interfaces* (Elsevier, Amsterdam, 1998)
2. M.A. Bos, T. van Vliet, *Adv. Colloid and Interface Sci.* **91**, 437 (2001)
3. B.S. Murray, *Current Opinion in Colloid & Interface Sci.* **7**, 426 (2002)
4. F. MacRitchie, *Adv. Colloid and Interface Sci.* **25**, 341 (1986)
5. P. Cicuta, I. Hopkinson, *J. Chem. Phys.* **114**, 8659 (2001)
6. P. Cicuta, I. Hopkinson, *Europhys. Lett.* **68**, 65 (2004)
7. F. Monroy, H.M. Hilles, F. Ortega, R.G. Rubio, *Phys. Rev. Lett.* **91**, 268302 (2003)
8. H.M. Hilles, F. Ortega, R.G. Rubio, F. Monroy, *Phys. Rev. Lett.* **92**, 255503 (2004)
9. R.A.L. Jones, R.W. Richards, *Polymers at Surfaces and Interfaces* (Cambridge Univ. Press, Cambridge (UK), 1999)
10. R. Miller, R. Wüstneck, J. Krägel, G. Kretzschmar, *Colloids and Surfaces A* **111**, 75 (1996)
11. M. Joly, *Rheological properties of monomolecular films*, in *Surface and Colloid Science*, Vol. 5, edited by E. Matijević (Wiley, New York, 1969)
12. D.M.A. Buzza, C.-Y.D. Lu, M.E. Cates, *J. Phys. II France* **5**, 37 (1995)
13. J. Benjamins, J.A. de Feijter, M.T.A. Evans, D.E. Graham, M.C. Phillips, *Faraday Discuss.* **59**, 218 (1975)
14. P. Cicuta, E.J. Stancik, G.G. Fuller, *Phys. Rev. Lett.* **90**, 236101 (2003)
15. G.T. Gavranovic, G.G. Fuller, to appear *Faraday Discuss.* **129**, 1 (2005)
16. A. Martin, M.A. Bos, M. Cohen Stuart, T. van Vliet, *Langmuir* **18**, 1238 (2002)
17. C.F. Brooks, G.G. Fuller, C.W. Curtis, C.R. Robertson, *Langmuir* **15**, 2450 (1999)
18. C. Barentin, C. Ybert, J.-M. di Meglio, J.-F. Joanny, *J. Fluid Mech.* **397**, 331 (1999)
19. J.T. Petkov, T.D. Gurkov, B.E. Campbell, R.P. Borwankar, *Langmuir* **16**, 3703 (2000)
20. G.L. Gaines, *Insoluble Monolayers at Liquid-Gas Interfaces* (Wiley, New York, 1960)

21. D.E. Graham, M.C. Phillips, *J. Coll. Interface Sci.* **76**, 227 (1980)
22. J. Lucassen, M. van den Tempel, *J. Coll. Interface Sci.* **41**, 491 (1972)
23. P.-G. de Gennes, *Scaling Concepts in Polymer Physics* (Cornell University Press, Ithaca, 1979)
24. R. Vilanove, F. Rondelez, *Phys. Rev. Lett.* **45**, 1502 (1980)
25. T.G. Mason, D.A. Weitz, *Phys. Rev. Lett.* **75**, 2770 (1995)
26. M.J. Ridout, A.R. Mackie, P.J. Wilde, *J. Agric. Food Chem.* **52**, 3930 (2004)
27. E.M. Freer, K.S. Yim, G.G. Fuller, C.J. Radke, *J. Phys. Chem. B* **108**, 3835 (2004)
28. P. Cicuta, I. Hopkinson, *Colloids and Surfaces A: Physicochem. Eng. Aspects* **233**, 97 (2004)
29. F. Sciortino, *Nature Materials* **1**, 145 (2002)
30. L. Santen, W. Krauth, *Nature* **405**, 550 (2000)
31. B.S. Murray, *Colloids and Surfaces A: Physicochem. and Eng. Aspects* **125**, 73 (1997)
32. E.H. Lucassen-Reynders, V.B. Fainerman, R. Miller, *J. Phys. Chem. B* **108**, 9173 (2004)
33. E. Dickinson, Y. Matsumura, *Colloids Surf. B: Biointerfaces* **3**, 1 (1994)
34. R.J. Green, I. Hopkinson, R.A.L. Jones, *Langmuir* **15**, 5102 (1999)
35. C.M. Wijmans, E. Dickinson, *Langmuir* **14**, 7278 (1998)
36. F. Monroy, F. Ortega, R.G. Rubio, *Eur. Phys. J. B* **13**, 745 (2000)